Effect of Root Architecture on Structural Stability and Erodibility of Topsoils during Concentrated Flow in Hilly Loess Plateau

LI Qiang[1, 3], LIU Guobin[1, 2], ZHANG Zheng[2], TUO Dengfeng[2], XU Mingxiang[1, 2]

(1. *State Key Laboratory of Soil Erosion and Dry Land Farming, Institute of Soil and Water Conservation, Chinese Academy of Sciences and Ministry of Water Resources, Yangling* 712100, *China*; 2. *Institute of Soil and Water Conservation, Northwest A&F University, Yangling* 712100, *China*; 3. *University of Chinese Academy of Sciences, Beijing* 100049, *China*)

Abstract: Traditional vegetation techniques for the control of concentrated flow erosion are widely recognized, whereas only a few studies have experimentally investigated the impacts of belowground roots on the erodibility of topsoils in semi-arid areas. To quantify the effects of root architectures on soil erodibility and its relevant structural properties, simulated flow experiments were conducted at six-week intervals from 18 July to 20 October in 2012 in the hilly Loess Plateau. Five treatments were: 1) bare (control), 2) purple alfalfa (*Medicago sativa*), representing tap roots (T), 3) switchgrass (*Panicum virgatum*), representing fibrous roots (F), 4) purple alfalfa and switchgrass, representing both tap and fibrous roots (T + F), and 5) natural recovery (N). For each treatment, soil structural properties and root characteristics were measured at an interval of six weeks. Soil anti-scouribility was calculated. Results showed that grass planting slightly reduced soil bulk density, but increased soil aggregate content by 19.1%, 10.6%, 28.5%, and 41.2% in the treatments T, F, T + F, and N, respectively. Soil shear strength (cohesion and angle of internal friction (φ)) significantly increased after the grass was planted. As roots grew, soil cohesion increased by 115.2%–135.5%, while soil disintegration rate decreased by 39.0%–58.1% in the 21th week compared with the recorded value in the 9th week. Meanwhile, root density and root surface area density increased by 64.0%–104.7% and 75.9%–157.1%, respectively. No significant differences in soil anti-scouribility were observed between the treatments of T and F or of T + F and N, but the treatments of T + F and N performed more effectively than T or F treatment alone in retarding concentrated flow. Soil aggregation and root surface-area density explained the observed soil anti-scouribility during concentrated flow well for the different treatments. This result proved that the restoration of natural vegetation might be the most appropriate strategy in soil reinforcement in the hilly Loess Plateau.

Keywords: fibrous roots; tap roots; root density; soil structural properties; soil anti-scouribility; hilly Loess Plateau; China

1 Introduction

In semi-arid areas, soil erosion is a serious threat to land productivity and sustainability for natural and human-managed ecosystems (Su *et al*., 2010; Fu *et al*., 2011; Zhang Lihua *et al*., 2012; Lian *et al*., 2013). Traditional vegetation techniques are recognized as effectively in reducing soil erosion, whereas the most evident vegetation source that protects soil against erosion is root reinforcement (Zhang *et al*., 2011; Reinhart *et al*., 2012). Root-permeated soils are generally more capable of withstanding soil erosion than plain soils mainly because of the physical enlacing and biochemistrical exudates of roots (Liu *et al*., 1998; Gyssels *et al*., 2003).

Grass planting on abandoned or rehabilitated land is a priority for the restoration in the hilly Loess Plateau (Fu and Peng, 2000; Zhang C *et al*., 2012). The reinforcement of soil by grass roots mainly depends on several variables such as root system morphology and mechanical architectures (Gyssels *et al*., 2003; Glab and Kacorzyk, 2011). Root architecture can significantly change the distribution of stresses and plastic strains within the soil medium as well as affect the resistance to scouring (De Baets *et al*., 2006). Several root parameters (root density, root dry weight, root length density, root surface area density, root area ratio) were used to describe the root effect, but the results of most studies showed that root architecture plays the most important role in the erosion resistance of the top soil to concentrated flow, and tap roots reduce the erosion rates to a lesser extent compared with fine-branched roots and that a root system composed of tap roots and fibrous roots would be ideal for reinforcing the soil against erosion (De Baets *et al*., 2007; Genet *et al*., 2008; Wang and Zhang, 2010). However, only a few studies have experimentally investigated the impacts of grass roots with different architectures on the erodibility of topsoils, which relies on soil anti-scouribility in the concentrated flow erosion zones of the Loess Plateau (Zhang *et al*., 2004; Zhou and Shangguan, 2005). Such information is essential for diagnosing a viable soil erosion control technique considering root architectures. Therefore, this study aims to experimentally investigate the impacts of root architectures on soil anti-scouribility and its relevant structural properties on a yearly basis.

2　Materials and Methods

2.1　Experimental design

This study was conducted in the Ansai Field Experiment Station (36°51′22″N, 109°18′52″E) of Chinese Academy of Sciences, Northwest China. Mean annual temperature and precipitation are 8.8℃ and 505.3 mm, respectively. This area is known for its erosion rate of approximately 10 000 t/(km²·yr) (Cai, 2001). The experiment site is located close to the top of the loess mounds with a slope gradient of 17°. In 2001, this site was naturally abandoned but was again converted into cropland in 2009. Early in May 2012, five plots measuring 9 m × 3 m (length × width) were established on the cropland. To improve the accuracy of measurement, each plot was

divided into three subplots sized 9 m × 1 m (length × width). The typical surface-soil properties are: clay content (< 2 μm) 9.3%, silt content (2–50 μm) 57.4%, sand content (50 μm–2 mm) 33.3%, and soil organic matter 3.77 g/kg. Purple alfalfa (*Medicago sativa*) represents tap roots, and switchgrass (*Panicum virgatum*) represents fibrous roots. The vegetation are recognized as effectively in reducing soil erosion, whereas the most evident vegetation source that protects soil against erosion is root reinforcement. Therefore, five treatments with three replicates considered were: 1) bare (control), 2) purple alfalfa, representing tap roots ((T), 251 plants/m²), 3) switchgrass, representing fibrous roots ((F), 157 plants/m²), 4) purple alfalfa and switchgrass ((T + F), 197 plants/m²), and 5) natural recovery ((N), 166 plants/m²). The main species under the natural recovery are herbs of Chinese pennisetum (*Setaira viridis* (L.) *Beauv*). Weeds growing on the grass plots and lichen crusts on the bare land were immediately cleared by using a biological herbicide during the early growing phase. Within all plots, a fine seedbed was manually established by crushing soil aggregates into a diameter lower than 1 cm. All plots were treated equally and received the same amount of rainwater. The grass seeds were sown randomly. This random sowing procedure was selected to mitigate the influence of sowing orientation.

2.2　Soil sample collection and flume experiment

Laboratory-simulated flow experiments, which began nine weeks after the grass was planted, were conducted at six-week intervals. The first samples were taken on 18 July 2012, and the last ones on 20 October 2012. Once the fields for sampling in each subplot were identified, the aboveground biomass was chipped to be level to the soil surface, and the residues were cleared. Two special rectangular sampling metal boxes with dimensions of 20 cm × 10 cm × 10 cm (length × width × depth) were driven into the soil by using a hammer. A wooden plank was placed on top of the metal box during hammering for protection. To extract the soil sample from the plot, some soil was dug out with a trowel from the area surrounding the metal box. The soil sample was then lifted in such a way that some soil was sticking out below the open bottom side of the sample. A total of 20 soil samples for flow experiments were taken from topsoil (0–10 cm). Thereafter, the sampling box was packed using a membrane with a plastic plate attached

to the bottom to prevent soil loss during transport. The undisturbed soil samples were taken to the laboratory and placed in a water bath for slow capillary rise for 12 h. The samples were then taken out of the water to drain for 8 h to obtain the same soil moisture before the experiment.

A concentrated flow experiment was conducted with a hydrological flume (length = 2.00 m, width = 0.10 m) similar to the one described by Zhou and Shangguan (2005) in Fig. 1. The flume contained an opening at its lower base. The opening was equal to the size of the sampling box such that the soil surface of the sample was at the same level as the flume surface. The space between the sample box and the flume edges was sealed with mastic of painter to prevent edge effects. The simulated runoff flux was designed according to the maximum potential runoff yield caused by a typical medium storm in the hilly Loess Plateau (2 mm/min) on a standard plot (20 m × 5 m). The flume slope was 15° referring to the standard of conversion from farmland to forestland in China. The scouring time was set at 15 min, which is the maximum time frequency for rainstorms in the study area. During the 15 min duration of each experiment, samples of runoff and detached soil were collected every 1 min during the first 3 min and every 2 min thereafter by using 10 L buckets. After the

suspended particles had settled, the clear water was drained off, and the sediments were sampled and oven-dried at 105℃.

Immediately after each flow experiment, all roots were separated from the soil samples by hand washing on a sieve. Each root segment was dried with filter paper and then placed on a rectangular transparent plastic paper. Overlap was avoided to minimize error. Afterwards, the roots on the plastic paper were scanned at a resolution of 300 dpi to obtain the root images for calculating root surface area density (RSAD, cm^2/cm^3). Staining was performed using methylene blue, with a contact time of 18 h, to visualize the roots better during image analysis (De Baets *et al*., 2006). Root density (RD, kg/m^3) is expressed by the dry mass of living roots divided by the volume of the root-permeated soil sample.

$$RD = \frac{M_D}{V} \qquad (1)$$

where M_D is dry mass of living root (kg), and V is volume of the sample box (m^3).

2.3 Soil indicator determination

Soil bulk density was determined using a soil core (height and diameter in 5 cm) at each sampling (Jia *et*
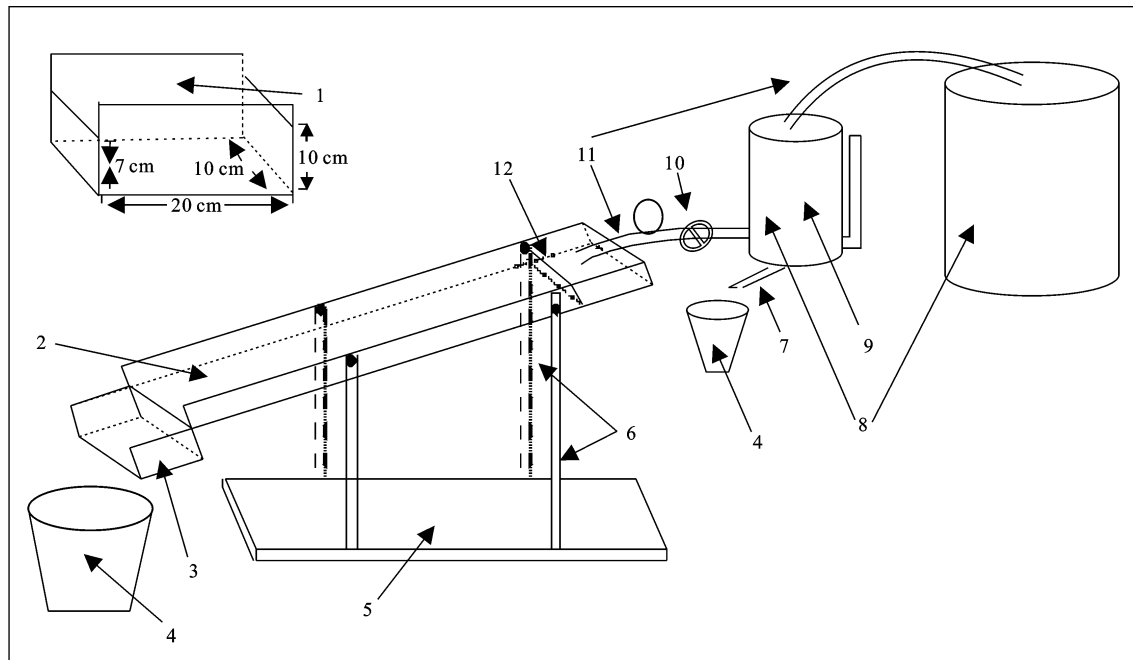

Fig. 1 Schematic diagram of experimental set-up. 1, sampling box; 2, scouring flume; 3, chamber for soil samples; 4, plastic bucket; 5, pedestal and bracket; 6, support for adjusting the gradient; 7, surplus water outlet; 8, storage reservoir; 9, glass pipe; 10, stopcock; 11, water-supply pipe; 12, water buffer chamber

al., 2005). Soil aggregate content was determined with a conventional wet sieving method (Yoder, 1936). Soil mean weight diameter (MWD) was calculated by using Equation (2) (Van Bavel, 1949).

$$MWD = \sum_{i=1}^{n}(\bar{R}_i W_i) \Big/ \sum_{i=1}^{n} W_i \qquad (2)$$

where $\bar{R}_i$ and W_i are the average diameter of the *i*th class soil aggregates and the percent of *i*th class in the bulk soil, respectively. Soil disintegration rate was measured with the can buoy method (Jiang *et al*., 1995). Direct shear strength samples were sealed at 4℃ after removal from the field. Samples were placed in a shear testing device, and four levels of loads (100 N, 200 N, 300 N, and 400 N) were applied as weights on separate samples. A lateral displacement was applied at a speed of 0.8 mm/min until failure occurred and the peak shear force was recorded. Soil cohesion and angle of internal friction (φ) were obtained based on the Mohr-Coulomb theory (Schuppener, 1999). Soil anti-scouribility (AS, L/g) was calculated as follows:

$$AS = \frac{f \times t}{W} \qquad (3)$$

where f is the flow rate (L/min), t is the scouring time (min), and W is the weight of oven-dried sediment (g).

2.4　Statistical analysis

Analysis of variance (ANOVA) was performed to determine the effects of roots with different architectures on soil structural stability and soil AS. SPSS 13.0 software and the least significant difference test ($p < 0.05$, two-tailed test) were used for data analysis.

3　Results and Discussion

3.1　Soil properties and root characteristics in different treatments

Table 1 shows the changes in soil structural properties and root characteristics under different treatments. As depicted in Table 1, a slight reduction in soil bulk density was observed after grass was planted, compared with the control. Among the treatments, on average, the largest decrease of 4.1% for soil bulk density was observed in the T treatment. Compared with recorded values in the 9th week, the soil bulk density in treatments T, F, T + F, and N during the 21th week were averagely reduced by 3.3%, 4.1%, 2.5%, and 4.8%, respectively. This finding was demonstrated in the study of Burylo *et al*. (2011), where the roots could promote water entry and soil aeration, thus decreasing soil bulk density.

Soil aggregate content is an index of soil erodibility because more aggregates are less prone to erosion, and higher proportions of fine particles improve flocculation and aggregation (Dai *et al*., 2007). On average, compared with the control, soil aggregate content during the 9th week was increased by 19.1%, 10.6%, 28.5%, and 41.2% in treatments T, F, T + F and N, respectively. Compared with the recorded value during the 9th week, soil aggregate content increased by 93.2% in the N treatment during the 21th week.

Meanwhile, soil MWD significantly increased, particularly for the N treatment, with a maximal increment of 85.7% after grass was planted. This result may indicate that natural recovery could contribute to good soil structure either by physically binding soil particles into aggregates or by releasing various organic or inorganic substances into soil, and such changes ultimately increased soil aggregate stability and retard concentrated flow (Govers *et al*., 1990; Marquez *et al*., 2004).

With respect to soil shear strength (including cohesion and φ), significant increments were found in soil cohesion and φ compared with control. Specifically, the mean soil cohesion respectively increased by 255.0% and 265.0%, and the mean φ increased by 25.8% and 40.8% in treatments T + F and N. Among the different stages, soil cohesion increased by 115.2% and 135.5% in the 21th week when compared with the data gathered during the 9th week in treatments T + F and N. This result is in agreement with previous studies which showed that increased roots could provide additional soil cohesion and enhance soil resistance to concentrated flow erosion (Gogichaishvili, 2012).

Soil disintegration rate decreased by 8.2%–76.4% after grass was planted compared with control. The soil disintegration rate in four treatments decreased by 39.0%–58.1% during the 21th week compared with those during the 9th week. These reductions were considerably larger in T + F and N treatments in the 21th week when compared with the control, which indicated that the mixture of tap and fibrous roots was better than the treatment with T or F alone in terms of protecting soil from disintegrating.

Table 1 Changes in soil structural properties and root characteristics in different treatments (mean ± standard deviation)

Indicator	Treatment	Control	9 week	15 week	21 week
Bulk density (g/cm^3)	T	1.21 ± 0.02a	1.20 ± 0.06a	1.25 ± 0.05a	1.16 ± 0.02a
	F	1.21 ± 0.02a	1.23 ± 0.06a	1.18 ± 0.04a	1.18 ± 0.04a
	T + F	1.21 ± 0.02a	1.21 ± 0.04a	1.19 ± 0.03a	1.18 ± 0.02a
	N	1.21 ± 0.02a	1.24 ± 0.05a	1.19 ± 0.04a	1.18 ± 0.02a
Aggregation (g/kg)	T	96.9 ± 8.3b	115.4 ± 12.0b	121.2 ± 14.3ab	148.8 ± 10.4a
	F	96.9 ± 8.3c	107.2 ± 14.2c	137.4 ± 12.4b	187.5 ± 26.5a
	T + F	96.9 ± 8.3c	124.5 ± 15.7b	149.6 ± 19.2b	204.5 ± 16.2a
	N	96.9 ± 8.3d	136.8 ± 13.5c	171.3 ± 16.2b	264.3 ± 13.9a
MWD (mm)	T	1.47 ± 0.12b	1.99 ± 0.15a	1.57 ± 0.13b	1.69 ± 0.15ab
	F	1.47 ± 0.12b	2.16 ± 0.11a	2.15 ± 0.08a	2.33 ± 0.16a
	T + F	1.47 ± 0.12c	2.22 ± 0.23b	2.13 ± 0.09b	2.72 ± 0.23a
	N	1.47 ± 0.12c	2.14 ± 0.10b	2.33 ± 0.11b	2.73 ± 0.07a
Soil cohesion (kPa)	T	2.0 ± 0.17d	2.3 ± 0.12c	3.5 ± 0.14b	3.8 ± 0.13a
	F	2.0 ± 0.17d	2.5 ± 0.19c	4.3 ± 0.33b	4.9 ± 0.29a
	T + F	2.0 ± 0.17d	3.3 ± 0.11c	5.7 ± 0.45b	7.1 ± 0.56a
	N	2.0 ± 0.17c	3.1 ± 0.09b	5.6 ± 1.12a	7.3 ± 0.79a
φ (°)	T	22.41 ± 0.49b	21.23 ± 1.02b	29.71 ± 0.98a	28.08 ± 0.93a
	F	22.41 ± 0.49c	25.69 ± 1.11b	29.76 ± 1.49a	29.03 ± 1.10a
	T + F	22.41 ± 0.49b	21.56 ± 0.89b	29.26 ± 1.32a	28.19 ± 0.72a
	N	22.41 ± 0.49c	28.99 ± 1.07b	30.27 ± 1.01a	31.56 ± 1.12a
Disintegration rate (cm^3/min)	T	1.95 ± 0.09a	1.46 ± 0.92b	0.90 ± 0.24c	0.89 ± 0.07c
	F	1.95 ± 0.09a	1.79 ± 0.18a	0.75 ± 0.26b	0.75 ± 0.05b
	T + F	1.95 ± 0.09a	1.14 ± 1.03b	0.61 ± 0.09c	0.49 ± 0.03c
	N	1.95 ± 0.09a	1.02 ± 0.17b	0.47 ± 0.21c	0.46 ± 0.04c
RD (kg/m^3)	T	–	1.00 ± 0.04c	1.25 ± 0.07b	1.64 ± 0.11a
	F	–	1.01 ± 0.05c	1.43 ± 0.09b	1.91 ± 0.12a
	T + F	–	1.06 ± 0.06c	1.39 ± 0.08b	2.17 ± 0.14a
	N	–	1.11 ± 0.08c	1.44 ± 0.10b	2.22 ± 0.16a
RSAD (cm^2/cm^3)	T	–	0.29 ± 0.05b	0.44 ± 0.05a	0.51 ± 0.07a
	F	–	0.34 ± 0.04c	0.53 ± 0.04b	0.66 ± 0.03a
	T + F	–	0.28 ± 0.05c	0.58 ± 0.04b	0.72 ± 0.06a
	N	–	0.36 ± 0.04c	0.52 ± 0.10b	0.69 ± 0.05a

Notes: MWD, mean weight diameter; φ, angle of internal friction; RD, root density; RSAD, root surface-area density. T, F, T + F and N were treatments of tap, fibrous roots, mixture of tap and fibrous roots and natural recovery. '–' means that the date was observed in bare soil (control), but that did not exist root, so no value was obtained. Different lowercase letters between stages indicates significant at $p < 0.05$

Root wedging is an important mechanism where roots can bind soil together and tie weak surface soil layers into strong and stable subsurface layers (Adili *et al.*, 2012). Compared with recorded values during the 9th week, RD during the 21th week increased by 64.0%, 89.1%, 104.7%, and 100.0% in treatments T, F, T + F, and N, respectively. It showed that the T + F and N treatments could produce more roots, which conse-

quently provides additional soil cohesion while preventing channel incision (Prosser *et al.*, 1995).

The RSAD was a better indicator to quantify the relationship between roots and soil erosion (Zhou and Shangguan, 2005). In this study, compared with recorded values during the 9th week, the RSAD in the treatments T, F, T + F, and N during the 21th week increased by 75.9%, 94.1%, 157.1%, and 91.7%, respec-

tively. As the RSAD increases, the soil-contacting area of the roots becomes larger, and the enlacing and adherence of root exudates to soil particles retard scouring (Sandeep *et al.*, 2010).

3.2 Effect of root architecture on soil anti-scouribility

As a parameter for evaluating the soil anti-erosion capacity, soil AS is closely related to soil structural properties and root characteristics (Zhou and Shangguan, 2007). Roots can form a dense network that physically binds soil particles, thus creating a mechanical barrier to soil erosion (Fang *et al.*, 2008). Figure 2 shows that a remarkable increase in the soil AS occurred with root growth. Compared with the control (0.28 L/g), the average soil AS after grass was planted at three stages in treatments T, F, T + F, and N increased by 34.9%, 50.9%, 77.0%, and 80.4%, respectively. Compared with the results in the 9th week an increase of 21.9%–225.0% was found during the 21th week. Moreover, the treatments of T + F and N were noted to perform more effectively than T or F treatment alone in terms of retarding concentrated flow, but no significant differences were observed between the T and F treatments or the T + F and N treatments. This finding is consistent with previous studies reporting that fine roots (≤ 1 mm) could exert stronger tensile strength and promote more cohesion and surface roughness (Prosser *et al.*, 1995). In addition, roots release various organic and inorganic substances into soil, which can improve the physical properties of soil around the roots. Therefore, additional studies that focus on the contributions of physical enlacing and biochemistrical exudates of roots to soil

AS under both natural and laboratory conditions might represent a more conclusive report.

3.3 Root contribution to soil loss reduction

As shown in Fig. 3, sediment loss was assumed to be constant (9.86 kg/m^2) within the three stages in the bare plot (control). The average sediment loss after the grass was planted in the treatments T, F, T + F, and N decreased by 36.1%, 47.3%, 106.2%, and 133.5%, respectively, as compared with that in the control. This result is consistent with previous studies that reported that grass planting was capable of reducing soil loss by 58%–98% compared with that in cropland (Zhou and Shangguan, 2007).

Compared with the sediment loss in the 9th week, a percentage of 70.0%–87.8% decrease was observed among different treatments during the 21th week. The most significant reduction appeared in the T + F and N treatments, mainly because the increased roots provided more barriers to surface flow and prevented sediment loss (Fang *et al.*, 2008). Similar results have been proven by field measurement and simulated concentrated flow experiments (De Baets *et al.*, 2006; Zhou *et al.*, 2010).

3.4 Correlation of soil AS and soil structural properties and root characteristics

Soil AS is a comprehensive indicator that depends on several factors such as soil aggregate content, soil shear strength and plant roots. Therefore, a step-wise regression analysis was carried out, and linear regression equations between soil AS and soil aggregate content, disintegration rate and RSAD are well correlated as follows:
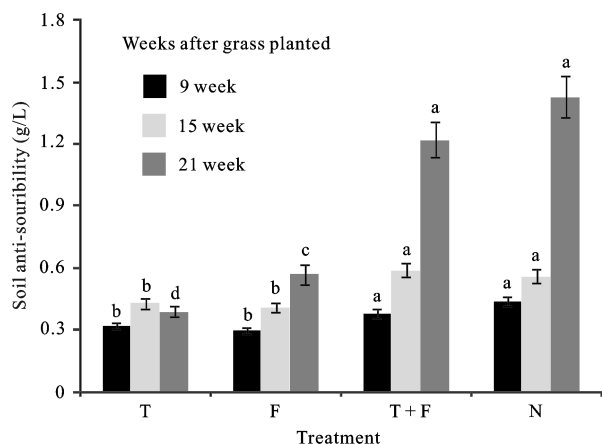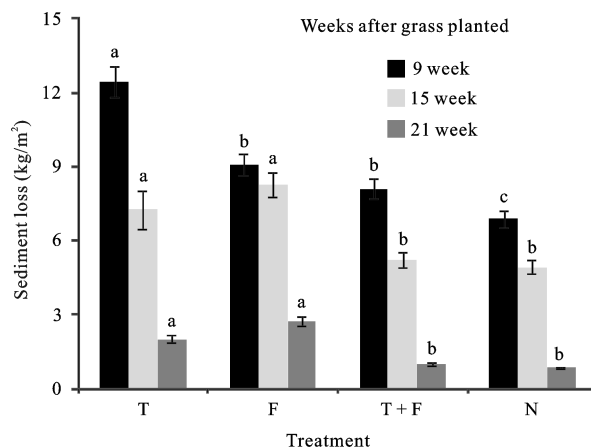

Fig. 2 Soil anti-scouribility (AS) in different treatments. T, F, T + F and N are treatments of tap, fibrous roots, both tap and fibrous roots and natural recovery. Different lowercase letters within same stage indicates significant at *p* < 0.05

Fig. 3 Sediment loss within scouring time in different treatments. T, F, T + F and N were treatments of tap, fibrous roots, mixture of tap and fibrous roots, and natural recovery. Different lowercase letters within same stage indicates significance at *p* < 0.05

$$\hat{Y} = 0.801SAC - 0.561SDR + 0.652RSAD - 0.315$$
$$(R^2 = 0.788, \ n = 16, \ p < 0.05) \tag{4}$$

The result showed that soil aggregation content and RSAD were the key positive indicators, contributing 71.8% to the reinforcement of soil AS in surface soil layer. However, soil disintegration rate was the main negative indicator, accounting for 29.2% of the reinforcement of the soil AS. Consistent with the findings of previous studies (Gyssels *et al.*, 2002; Zhou and Shangguan, 2005), these results suggested that the soil AS could be effectively reinforced by increasing the soil-contacting area of the roots and ameliorating soil structural properties. The results also showed that the improvement in soil structural properties and root characteristics was the primary reason for enhancing the soil AS. Thus, soil aggregation and root surface-area density explain the observed soil AS during concentrated flow well for the different treatments.

4 Conclusions

Root architecture significantly affects soil structural properties and the soil AS. Compared with bare land, grass planting reduces sediment loss by 36.1%–133.5%. A slight reduction occurs in soil bulk density, while significant increments of 19.1%, 10.6%, 28.5%, and 41.2% in soil aggregate content are observed in treatments T, F, T + F, and N, respectively. Soil cohesion and φ increased significantly after grass is planted. Among the different stages, soil cohesion increases by 115.2%–135.5%, while soil disintegration rate decreases by 39.0%–58.1% during the 21th week when compared with the recorded data during the 9th week. Meanwhile, the RD and RSAD increases by 64.0%–104.7% and 75.9%–157.1%, respectively. The treatments of T + F and N perform more effectively than T or F treatment alone in terms of retarding concentrated flow, but no significant differences in the soil AS were identified between T + F and N. Soil aggregation and root surface-area density explain the observed soil AS during concentrated flow well for the different treatments. Thus, restoration of natural vegetation in the Loess Plateau is a priority to achieve an enhanced capacity to resist soil erosion on a yearly basis. Therefore, a long-term location experiment should be conducted referring to the differences in soil chemical and biological properties associated with soil AS.

References

Adili A A, Azzam R, Spagnoli G *et al*., 2012. Strength of soil reinforced with fiber materials (Papyrus). *Soil Mechanics and Foundation Engineering*, 48(6): 241–247. doi: 10.1007/s11204-012-9154-z

Burylo M, Hudek C, Rey F, 2011. Soil reinforcement by the roots of six dominant species on eroded mountainous marly slopes (Southern Alps, France). *Catena*, 84(1–2): 70–78. doi: org/10.1016/j.catena.2010.09.007

Cai Q G, 2001. Soil erosion and management on the Loess Plateau. *Journal of Geographical Sciences*, 11(1): 53–70. doi: 10.1007/BF02837376

Dai Quanhou, Liu Guobin, Xue Sha *et al*., 2007. Dynamics of soil water stable aggregates and relationship with soil properties on abandoned arable land in eroded hilly Loess Plateau. *Journal of Soil and Water Conservation*, 21(2): 61–64, 77. (in Chinese)

De Baets S, Poesen J, Gyssels G *et al*., 2006. Effects of grass roots on the erodibility of topsoils during concentrated flow. *Geomorphology*, 76(1–2): 54–67. doi: org/10.1016/geomorph.2005.10.002

De Baets S, Poesen J, Knapen A *et al*., 2007. Impact of root architecture on the erosion-reducing potential of roots during concentrated flow. *Earth Surface Process Landforms*, 32(9): 1323–1345. doi: 10.1002/esp.1470

Fang C, Li X W, Zhang J *et al*., 2008. Biomass of fine roots and its relationship with water-stable aggregates in a composite ecosystem of triploid Populus tomentosa in the conversion of farmland to forest. *Frontiers of Forestry in China*, 3(2): 158–164. doi: 10.1007/s1146-008-0031-x

Fu B J, Liu Y, Lyu Y H *et al*., 2011. Assessing the soil erosion control service of ecosystems change in the Loess Plateau of China. *Ecoogical Complexity*, 8(4): 284–293. doi: org/10.1016/j.ecocom.2011.07.003

Fu Chen, Peng Buzhuo, 2000. The effect of land use changes on soil conditions in arid region. *Chinese Geographical Science*, 10(3): 226–230. doi: 10.1007/s1169-000-0005

Genet M, Kokutse N, Stokes A *et al*., 2008. Root reinforcement in plantations of Cryptomeria japonica D. Don: Effect of tree age and stand structure on slope stability. *Forest Ecological Management*, 256(8): 1517–1526. doi: 10.1016/j.foreco.2008.05.050

Glab T, Kacorzyk P, 2011. Root distribution and herbage production under different management regimes of mountain grassland. *Soil Tillage Research*, 113(2): 99–104. doi: org/10.1016/j.still.2011.02008

Gogichaishvili G P, 2012. Erodibility of arable soils in Georgia during the period of storm runoff. *Eurasian Soil Science*, 45(2): 189–193. doi: 10.1134/s106422931202010x

Govers G, Everaert W, Poesen J *et al*., 1990. A long flume study of the dynamic factors affecting the resistance of a loamy soil to concentrated flow erosion. *Earth Surface Process Landform*, 15(4): 515–524. doi: 10.1002/esp. 3290150403

Gyssels G, Poesen J, Bochet E *et al*., 2003. The importance of plant root characteristics in controlling concentrated flow erosion rates. *Earth Surface Process Landforms*, 28(4): 371–384. doi: 10.1002/esp.447

Gyssels G, Poesen J, Nachtergaele J *et al*., 2002. The impact of sowing density of small grains on rill and ephemeral gully erosion in concentrated flow zones. *Soil Tillage Research*, 64(3): 189–201. doi: org/10.1016/j.still.2002.02008

Jia G M, Cao J, Wang C Y *et al*., 2005. Microbial biomass and nutrients in soil at the different stages of secondary forest succession in Ziwulin, Northwest China. *Forest Ecology and Management*, 217(1): 117–125. doi: 10.1016/j.foreco.2005.05.055

Jiang Dingsheng, Li Xinhua, Fan Xingke *et al*., 1995. Research on the law of soil disintegration rate change and it′s effect factors on the Loess Plateau. *Bulletin of Soil and Water Conservation*, 15(3): 20–27. (in Chinese)

Lian Jie, Zhao Xueyong, Zuo Xiao′an *et al*., 2013. Land cover changes and the effects of cultivation on soil properties in Shelihu wetland, Horqin Sandy Land, Northern China. *Journal of Arid Land*, 5(1): 71–79. doi: 10.1007/s40333-013-0143-5

Liu Guobin, 1998. Study on soil anti-scouribility and its mechanism. *Journal of Soil and Water Conservation*, 4(1): 93–96. (in Chinese)

Marquez C O, Garcia V J, Cambardella C A *et al*., 2004. Aggregate-size stability distribution and soil stability. *Soil Science Society of America Journal*, 68(3): 725–735. doi: 10.2136/222aj2004.7250

Prosser I P, Dietrich W E, Stevenson J, 1995. Flow resistance and sediment transport by concentrated overland flow in a grassland valley. *Geomorphology*, 13(1–4): 71–86. doi: org/10.1016/0169-555x(95)00020-6

Reinhart K O, Johnson D, Clay K, 2012. Conspecific plant-soil feedbacks of temperate tree species in the southern Appalachians, USA. *PLOS ONE*, 7(7): 1–7. doi: 10.1371/journal.pone.0040680

Sandeep K, Udawatta R P, Anderson S H, 2010. Root length density and carbon content of agroforestry and grass buffers under grazed pasture systems in a Hapludalf. *Agroforestry Systems*, 80(1): 85–96. doi: 10.1007/s10457-010-9312-0

Schuppener, 1999. *Laboratory Method for Direct Shear Tests. Recommendation of the ISSMGE for Geotechnical Testing.* Gemany: Beuth Verlag GmbH, 87–92.

Su Z A, Zhang J H, Nie X J, 2010. Effect of soil erosion on soil properties and crop yields on slopes in the Sichuan Basin, China. *Pedosphere*, 20(6): 736–746. doi: org/10.1016/s1002-0160(10)60064-1

Van Bavel C H M, 1949. Mean weight diameter of soil aggregates as a statistical index of aggregation. *Soil Science Society of America Journal*, 14(C): 20–23.

Wang Junming, Zhang Xinchang, 2010. Vertical distribution of root in different successional stages of grassland on abandoned cropland. *Science Soil and Water Conservarion*, 8(4): 67–72, 85. (in Chinese)

Yoder R E, 1936. A direct method of aggregate analysis of soils and study of the physical nature of soil erosion losses. *Agronomy Journal*, 28(5): 337–351.

Zhang C, Liu G B, Xue S *et al*., 2012. Rhizosphere soil microbial properties on abandoned croplands in the Loess Plateau, China during vegetation succession. *European Journal of Soil Biology*, 50: 127–136. doi: org/10.1016/j. ejsobi. 2012.01.002

Zhang G H, Liu G B, Wang G L *et al*., 2011. Effect of vegetation cover and rainfall intensity on sediment-bound nutrient loss, size composition and volume fractal dimension of sediment particles. *Pedosphere*, 21(5): 676–684. doi: org/10.1016/s1002-0160(11)60170-7

Zhang K L, Li S, Peng W, 2004. Erodibility of agricultural soils on the Loess Plateau of China. *Soil and Tillage Research*, 76(2): 157–165. doi: org/10.1016/j.still.2003.09.007

Zhang Lihua, Xie Zhongkui, Zhao Ruifeng *et al*., 2012. The impact of land use change on soil organic carbon and labile organic carbon stocks in the Longzhong region of Loess Plateau. *Journal of Arid Land*, 4(3): 241–250. doi: 10.3724/SP.J.1227.2012.00241

Zhou Z C, Gan Z T, Shangguan Z P *et al*., 2010. Effects of grazing on soil physical properties and soil erodibility in semiarid grassland of the northern Loess Plateau. *Catena*, 82(2): 87–91. doi: org/10.1016/j. catena. 2010. 05. 005

Zhou Z C, Shangguan Z P, 2005. Soil anti-scouribility enhanced by plant roots. *Journal of Integrative Plant Bioogy*, 47(6): 676–682. doi: 10.1111/j.1744-7909.2005.00067.x

Zhou Z C, Shangguan Z P, 2007. The effects of ryegrass roots and shoots on loess erosion under simulated rainfall. *Catena*, 70(3): 350–355. doi: org/10.1016/j.catena.2006.11.002